J Vet Clin 24(2) : 208-213 (2007)

Journal of Veterinary Clinics
www.ksvc.or.kr

Assessment of Systemic Arterial Thromboembolism with Multi-Slice Spiral CT in a Dog

Seung Ho Shin and Ki-Chang Lee[1]

College of Veterinary Medicine, ChonBuk National University 664-14 duckjin-dong, Jeonju, 561-756, Republic of Korea

(Accepted: March 15, 2007)

Abstract : A 15 kg 6-year-old intact male Jindo dog with a history of a respiratory distress, hindlimb paralysis with necrosed skin of dorsal digit for three weeks was referred to Animal Medical Center, Chonbuk National University. Heartworm infection was identified by kit examination. In plain thoracic radiographs, dilated pulmonary arteries reverse D sign and focal interstitial pattern was compatible with heartworm infection and possible pulmonary thromboembolism. Abdominal radiographs showed poor serosal detail indicating fluid accumulation within peritoneal cavity. No evidence of musculoskeletal abnormalities was found. Ultrasonography presented focal wedge-shaped hyperechogenecity on the both poles of left kidney, weak or absent pulse on the distal to the external iliac artery as well as ascites and irregular liver margin. Multi-organ failure was strongly supposed by blood profile including leukocytosis, anemia, hemoglobinuria bililubinemia, hypoalbuminemia, imbalance of electrolytes, and increased hepatic and renal function values. Interestingly, the glucose level is remarkably lower in pelvic limb compared to thoracic limb. Suspected pulmonary thromboembolism, renal infarction and femoral arterial embolization causing hindlimb paralysis and dermatic necrosis were confirmed by 3D reconstructed CT imaging. Prior to taking a consideration of euthanasia, interventional radiology was experimentally attempted but failed due to not recovered from general anesthesia. Early and accurate diagnosis of thromboembolism is valuable and 3D reconstructed CT images might be very useful to show the correct way to treat effectively.

Key words **:** 3D reconstructed CT, thromboembolism, heartworm, dog.

Introduction

Thromboembolic disease seems to be less common in dogs than it is in cats and humans. A retrospective study of canine necropsies over a 16-year period revealed that only 36 dogs out of a total of 8000 dogs could be diagnosed with aortic thromboembolism (35). Recently, only a case of femoral artery thrombosis in an immature dog was reported. It has been known that arterial thrombosis in the dog is related to the primary conditions such as hyperadrenocorticism, heart disease, protein-losing nephropathy, and neoplasia (4,5,28). This report includes femoral and pulmonary artery thrombosis in a dog with heart disease due to severe burden of heartworm infection.

Case

History and clinical findings

A 15 kg 6-year-old intact male Jindo weighing 18 kg presented to the Animal Medical Center (AMC), Chonbuk National University with the chief concern of inability to use its hind limbs since 3 weeks before. Hind limb paralysis, respiratory distress and necrosed skin of dorsal digit were observed. The dog was initially treated at a local veterinary hospital with bronchial dilator and prednisolone. And the cause of hind limb paralysis was comprehended. The dog was quite. Mucous membranes were pale pinky. Rectal temperature was 38.3°C, heart rate was 140 beats/minute (bpm), and respiratory rate was 60 breaths/minute. Physical examination revealed the following abnormalities: weak left and right femoral pulses and cyanotic nail beds on the hind paws. Deep pain perception was present in both hind limbs and no voluntary motor function was noted. A necrosed dorsal skin of both hind paws. The dog's problems included posterior paresis, weak femoral pulses with cyanotic nail beds and nocrosed paw's skin (Fig 1).

Differential diagnoses for the posterior paresis with lower motor neuron signs included an ischemic lesion of the spinal cord and neuropathy. Possible causes of the weak femoral pulses and cyanotic nail beds included hypovolemic shock and vascular compromise to the hind limbs.

Radiological and sonographic findings

Thoracic radiographs revealed distinct dilation of main pulmonary artery, enlarged cranial and caudal pulmonary arteries, reverse D sign and focal interstitial pattern on the caudal lung lobes were found and those radiographic findings were compatible with heartworm infection and possible pulmonary thromboembolism (Fig 2).

[1]Corresponding author.
E-mail : kclee@chonbuk.ac.kr

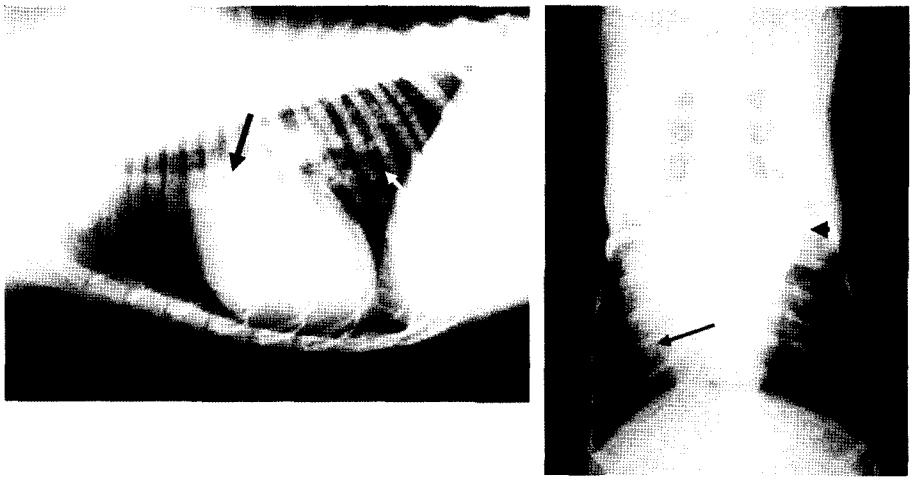

Fig 2. Thoracic radiographs revealed distinct dilation of main pulmonary artery (arrow), enlarged cranial and caudal pulmonary arteries (arrowhead), reverse D sign (small arrow) and focal interstitial pattern on the caudal lung lobes (white arrow).

Fig 1. The necrosed of the dorsal region of distal limbs were observed.

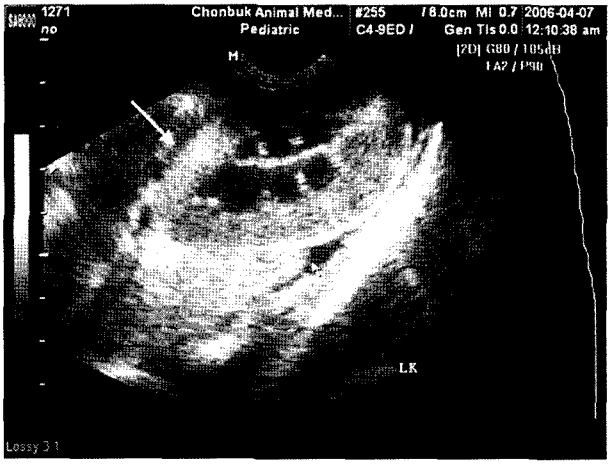

Fig 3. Longitudinal left renal sonogram. Note the irregular contour along with wedge shaped, hyperechoic appearance with a broader base at the surface of the left kidney that narrows toward the corticomedullary junction (arrow).

Abdominal radiographs showed lack of serosal detail representing fluid accumulated abdominal cavity. No evidence of musculoskeletal abnormalities was found. Ultrasonography displayed ascites, wedge-shaped hyperechogenecity on the left kidney (Fig 3) and weak or absent pulse on the femoral artery distal to the external iliac artery.

Hematological and serological findings

The blood work revealed the following, with standardized normal ranges for the AMC laboratory in parenthesis: WBC 35.3 × 10^3/μl (6.0-17.0 × 10^3/μl), packed cell volume 27% (37-54%), total bililubin 0.9 mg/dl (0.1-0.6 mg/dl), albumin 1.9 g/dl (2.5-4.4 g/dl), aspartate aminotransferase (AST) 216 U/L (7-84), blood urea nitrogen (BUN) 78 mg/dl (7-25 mg/dl), creatinine 2.1 mg/dl (0.4-1.5 mg/dl), phosphorus 8.4 mg/dl (2.7-8.0 mg/dl), Cl^- 121 mmol/L (87-120 mmol/L), Na^+ 137 mmol/L (140-165 mmol/L), and blood glucose 102 mg/dl for a forelimb, 71 mg/dl for a hind limb. Based upon the findings from diagnostic imaging combined with the blood profile, the differentials included renal ischemic injury, acute renal failure, hepatic failure and impaired blood circulation into the hind limbs causing posterior paresis and necrosed paw skin.

Conservative treatment

Fluid therapy with normal saline was applied to decrease the azotemia and correct imbalanced electrolytes. To prevent the formation of additional thrombi within the vasculature, the dog received heparin at a dose of 700 IU SQ q 24 hours. The dog was monitored in the critical care unit overnight.

Further study - CT findings

On the second day of hospitalization, CT scanning was performed to verify the degree and location of multiple lesions such as renal infarction, hepatic failure, pulmonary throm-

boembolism, and femoral arterial embolization.

Axial CT images combined with post processed 3D reconstructed images revealed clearly the suspected lesions. Complete obstruction of femoral arteries bilaterally (Fig 4), pulmonary thromboembolism on the right and left lung lobes (Fig 5), severe left renal infarction injury (Fig 6), cirrhotic changes of liver were apparent.

Fig 4. Femoral arterial thromboembolism on 3D reconstructed image of arterial phase CT scanning. No vessel was found distally from the femoral head level due to complete obstruction of femoral arteies bilaterally (arrows).

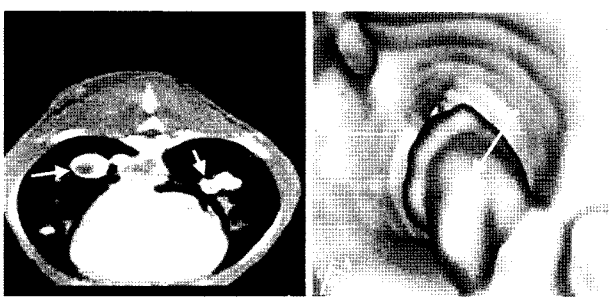

Fig 5. Thoracic CT image. A, Axial enhanced CT image show dilated pulmonary artery with hypoatteunated embolic material bilaterally (white arrows). B, Pulmonary arterial virtual endoscophic image revealed protruded embolic material within pulmonary artery (white arrow).

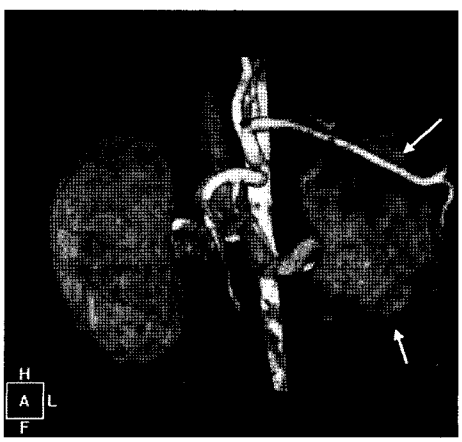

Fig 6. Renal 3D reconstructed CT image. Injured area by renal infarction was observed at the left kidney (arrows).

Outcome

The prognosis was considered grave though, interventional radiology was attempted to decrease or resolve the thrombi obstructing femoral arteries followed by pulmonary arteries experimentally under the consensus of patient's owner. The dog was dead to cardiac arrest during delivery the thrombi-resolution agent, Urokinase used widely for human.

Discussion

Thromboembolic disease is not common though, arterial occlusion has been reported in dogs occurring secondary to atherosclerosis, nephrotic syndrome, vegetative endocarditis, neoplastic emboli, dirofilariasis, trauma, and thrombi of left heart origin. Venous thrombosis frequently causes fewer clinical abnormalities than arterial thrombosis and consequently is frequently undetected (6,7,15,19,21,24,31,32). The distal aorta, iliac, renal, and femoral arteries are common sites of systemic thromboembolism (TE) (35).

Vascular thrombosis is most readily identified when arteries are affected, and the clinical consequences are generally acute and severe (22). Acute, complete arterial occlusion may cause posterior paresis, extreme hindlimb pain, and general distress (8,17). In some cases the animal may have an unsteady gait, lameness, progression to stumbling, weakness, or collapse. Pulmonary vascular obstruction can also result from thrombus formation, or embolization of thrombi, parasites, fat, or neoplastic cells.

The patient with serious burden of heartworm showed the clinical signs such as general distress, dyspnea and posterior paresis might be related with thromboembolism of pulmonary arteries and femoral arteries induced by heartworm itself or heartworm disease related matter.

Heartworm disease is the most common cause of Pulmonary thromboembolism (PTE) in dogs (16,25). Sudden onset respiratory distress and tachypnea are common historical or physical examination abnormalities seen in 50% to 96% of dogs and 55% of cats with PTE (21,29). Pulmonary thromboembolism (PTE) is a life-threatening condition that occurs in more than 600,000 human patients a year. Despite increased awareness and sophisticated imaging modalities in human medicine, only 30% of fatal PTE is diagnosed antemortem (33). Similarly, PTE was suspected antemotem in only 38% of dogs and 14% of cats with postmortem evidence of major PTE (16,25).

Physical examination may reveal cool distal limbs and swollen muscles. The cold and necrosed distal limbs were observed in this patient. It can be inferred that the throboembolic disease lasted for a long time in this case. Considering the history and clinical signs of the patient, peripheral and pulmonary

arterial TE are hypothetical diagnosis.

Confirmation of diagnosis may require proof of a vascular occlusion. This can be accomplished in some cases by physical examination, whereas in others, arteriography or diagnostic ultrasound are required (2,10,26).

When peripheral arterial thrombosis is suspected, a survey radiograph is indicated to evaluate cardiac size and shape and to assess for pulmonary changes including edema, thrombosis, or dirofilarasis. Chest and abdominal radiographs should be evaluated for orthopedic lesions, which could result in posterior paresis. In addition, radiographs of the pelvic and hindlimb region may be indicated to check for masses that could exert pressure on the aorta and for periosteal reactions in the sublumbar area. Cardiac enlargement with dilated pulmonary arteries, focal interstitial pattern were found and those radiographic findings were compatible with heartworm infection and possible: PTE. Thoracic radiographic abnormalities are common but are rarely specific for PTE. In fact, 10% to 30% of dogs and 14% of cats had normal thoracic radiographs despite necropsy proven PTE, which indicates that PTE should be a top differential diagnosis in an animal with marked respiratory distress and normal thoracic radiographs (16,25). Pulmonary infiltrates may be interstitial, alveolar, or lobar in dogs and cats (25).

Abdominal radiographs revealed poor serosal detail indicating ascites. No evidence of musculoskeletal abnormalities which are possible causes of posterior paresis was found. Ultrasound imaging provides a direct, noninvasive technique for assessing anatomic abnormalities, vascular patency, and function (10,35). Ultrasonography revealed ascites, irregular liver margin, and wedge-shaped hyperechogenecity on the bipolar region of the left kidney and weak or absent pulse on the femoral artery distal to the external iliac artery. These findings are compatible with the renal infarction and femoral arterial occlusion induced by TE.

Spiral CT and magnetic resonance (MR) angiography are noninvasive imaging modalities that show promise for the future diagnosis and management of PTE. To verify the occlusion of arterial vessels without high risk of general anesthesia, multi-slice CT scanning rather than angiography was performed in this dog with sedation. Pulmonary angiography is the gold standard for diagnosis of PTE in humans but is rarely used in veterinary medicine since general anesthesia is usually required, and patients with severe PTE and pulmonary hypertension are high-risk anesthetic candidates (2,30).

In this case, axial CT images combined with post processed 3D reconstructed images by multi slice spiral CT and software program exposed clearly the suspected lesions such as renal infarction and femoral and pulmonary arterial TE on radiography and ultrsonography. Complete obstruction of femoral arteries bilaterally, pulmonary thromboembolism on the right and left lung lobes, global renal infarction injury, and cirrhotic changes of liver were recognized apparently in this case. Renal infarcts can be reported either as focal or global on a basis of CT findings. The focal form of renal infarct is generally represented by a wedge-shaped area of low attenuation on an infusion CT scan. This form is most likely due to occlusion of small branches of the renal arteries. A global infarct is represented by a uniform area of low attenuation involving greater than 50 of the kidney and is usually due to occlusion of a major branch of the renal artery (1,3,11,12,13,14). CT findings on the renal revealed the degree and type of injury more in detail compared to sonographic findings.

Frequently, hepatorenal dysfunction also is observed in many dogs with caval syndrome induced by heartworm infection like in this case (9). Prognosis generally is poor unless the cause of the crisis-the right artrial and caval heartworms-is removed. Even with this treatment, mortality can approximate 40% (9). Although there are reports of successful thrombolytic therapy in experimental canine PTE in dogs with normal thrombolytic and anticoagulant systems (27) and in animals with systemic thrombi, there are no published studies evaluating thrombolytic therapy in naturally occurring PTE in veterinary medicine. And there is only one study regarding on the treatment of femoral arterial thrombosis in an immature dog (34).

Euthanasia is inevitable in this dog, however, surgical removal of heartworm followed by the treatment for femoral arterial TE, PTE with thrombolytic agents was attempted experimentally at the risk of cardiac arrest during the planed procedure. Thrombolytic agents such as streptokinase, urokinase, and tissue plasminogen activator (tPA) are potent activaors of fibrinolysis. These agents have used with variable and often limited success in veterinary medicine (5,8,18,28). Urokinase was determined to use for thrombolytic agent in this dog. Unfortunately, all the attempts were not made due to sudden death of the dog during the procedure under inhalation anesthesia and consensus of autopsy was not achieved.

Since precise and fast evaluation of thromboembolizm affecting pulmonary vessels and peripheral arteries is somewhat difficult in conventional modalities such as radiography and ultrsonography, the advanced methods like CT and MRI are essential for assessment of patient's status rapidly. Principally, multi slice spiral CT can be applied for evaluating vasculature disease quickly. Moreover, post processed 3D image can be contributed to assess the complicated disease with ease and precise. Therefore, femoral arterial thromboembolism causing hind limb paresis and pulmonary arterial thromboembolism disturbing the respiratory system could be determined easily and punctually by multi spiral CT scanning combined with 3D reconstructed images.

Acknowledgment

This paper was supported in part by 2nd stage Brain Korea 21 project in 2006.

References

1. Allibone GW. Renal infarction presenting as a mass. Diagnostic role of computed tomography and ultrasound. Urology

1982; 19: 98-100.
2. Bart Dolmatch, William J. Bavros, Thomas M. Grist. Diagnostic angiography. In: Peripheral Vascular Diseases, 2nd ed. St Louis, CV Mosby 1996: 65.
3. Berliner L, Redmond P, DeBalsi J. Renal infarction in bacterial endocarditis diagnosed by computed tomography. Urol Radiol 1982; 4: 231-233.
4. Boswood A, Lamb CR, White RN. Aortic and iliac thrombosis in six dogs. J Small Anim Prac 2000; 41: 109-114.
5. Clare AC, Kraje BJ. Use of recombinant tissue-plasminogen activator for artoic thrombolysis in a hypoproeinemic dog. J Am Vet Med Assoc 1998; 212: 539-543.
6. Cook AK, Cowgill LD. Clinical and pathological features of protein-losing glomerular disease in the dog: a review of 137 cases (1985-1992). 1996; 32: 313-322.
7. Dibartola SP, Tarr MJ, Parker AT, Powers JD, Pultz JA. Clinicopathologic findings in dogs with renal amyloidosis: 59 cases (1976-1986). J Am Vet Med Assoc 1989; 195: 358-364.
8. Fox PR, Sisson DD, Moise NS. Feline myocardial diseases. In: Canine and Feline Cardiology. New York, Churchill Livingstone 1988; pp 454-459.
9. Frank JR, Nutter FB, Kyles AE, Atkins CE, Sellon RK. Systemic arterial dirofilariasis in five dogs. J Vet Intern Med 1997; 11: 189-194.
10. Gareth W.L. Phillips, Review of Arterial Vascular Ultrasound, World Journal of Surgery 2000; 24: 232–240.
11. Glazer GM, Francis IR, Brady TM, Teng SS. Computed tomography of renal infarction: Clinical and experimental observation. AJR 1983; 140: 721-727.
12. Glazer GM, London SS. CT appearance of global renal infarction. J Comput Assist Tomogr 1981; 5: 847-850.
13. Haaga JR. Morrison SC. Case report-CT appearance of renal infarct. J Comput Asssist Tomogr 1980; 4: 246-247.
14. Harris RD, Dorros S. Computed tomographic diagnosis of renal infarction. Urologoy 1981; 17: 287-289.
15. Hogan DF, Dhaliwal RS, Sisson DD, Kitchell BE. Paraneoplastic thrombocytosis-induced systemic thromboembolism in a cat. J Am Anim Hosp Assoc. 1999; 35: 483-486.
16. Johnson LR, Lappin MR, Baker DC: Pulmonary thromboembolism in 29 dogs: 1985-1995, J Vet Intern Med 1999; 13: 338-345.
17. Joseph RJ, Greenlee PG, Carrillo JM, Kay WJ. Canine cerebrovascular disease–clinical and pathologic findings in 17 cases. JAAHA 1987; 24: 569-576.
18. Killingworth CR, Eyster GE, Adams T, Bartlett PC, Bell TG. Streptokinase treatment of cats with experimentally induced aortic thrombosis. Am J Vet Res. 1986; 47: 1351-1359.
19. Klein MK, Dow SW, Rosychuk RA, Pulmonary thromboembolism associated with immune-mediated hemolytic anemia in dogs. Ten cases (1982-1987). J Am Vet Med Assoc 1989; 195: 246-250.
20. Kweon JK, Song KJ, Lee KC, Lee HC and Choi MC. Computed Tomographic Charateristics of Nasal Squamous Cell Carcinoma in a Dog: J Vet Clin 2003; 20: 399-402.
21. LaRue MJ, Murtaugh RJ. Pulmonary thromboembolism in dogs: 47 cases (1986-1987). J Am Vet Med Assoc. 1990; 197: 1368-1372.
22. Laste NJ, Harpster NK. A retrospective study of 100 cases of feline distal aortic thromboembolism: 1977-1993. J Am Anim Hosp Assoc 1995; 31: 492-500.
23. Lee KC, Kweon JK, Song KJ and Choi MC. Three Dimensional ComputedTomography in the Assessment of Subtle Fracture in Dogs: J Vet Clin 2003; 20: 523-526.
24. Nichols R. Complications and concurrent disease associated with canine hyperadrenocorticism. Vet Clin North Am Small Anim Pract. 1997; 27: 309-320.
25. Norris CR, Griffey SM, Samii VF. Pulmonary thromboembolism in cats: 29 cases (1987-1997), J Am Vet Med Assoc 1999; 215: 1650-1654.
26. Polak JF. Peripheral arterial disease. Evaluation with color flow and duplex sonography. Radiol Clin North Am. 1995; 33: 71-90.
27. Prewitt RM, Hoy C, Kong A, Gu SA, Greenberg D, Cook R, Chan SM, Ducas J. Thrombolytic therapy in canine pulmonary embolism. Comparative effects of urokinase and recombinant tissue plasminogen activator, Am Rev Respir Dis 1990; 141: 290-295.
28. Ramsey CC, Bumey DP, Macintire DK, Finn-Bodner S. Use of streptokinase in four dogs with thrombosis. J Am Vet Med Assoc 1996; 209: 780-785.
29. Rawlings CA: Pulmonary vascular response of dogs with heartworm disease, Can J Comp Med 1978; 42: 452-459.
30. Rees CR, Palmaz JC, Garcia O, Alvarado R, Siegle RL. The hemodynamic effects of the administration of ionic and nonionic contrast materials into the pulmonary arteries of a canine model of acute pulmonary hypertension, Invest Radiol 1998; 23:184-189.
31. Ritt MG, Rogers KS, Tomas JS. Nephrotic syndrome resulting in thromboembolic disease and disseminated intravascular coagulation in a dog. J Am Anim Hosp Assoc. 1997; 33: 385-391.
32. Scott-Moncrieff JC, Treadwell NG, McCullough SM, Brooks MB. Hemostatic abnormalities in dogs with primary immune-mediated hemolytic anemia. J Am Anim Hosp Assoc 2001; 37: 220-227.
33. Stein PD, Terrin ML, Hales CA, Palevsky HI, Saltzman HA, Thompson BT, Weg JG. Clinical, laboratory, roentgenographic, and electrocardiographic findings in patients with acute pulmonary embolism and no pre-existing cardiac or pulmonary disease, Chest 1991; 100: 598-603.
34. Tater KC, Drellich S, Beck K. Management of femoral artery thrombosis in an immature dog. Journal of Veterinary Emergency and Critical Care 2005; 15: 52-59.
35. Van Winkle TJ, Hackner SG, Liu SM. Cinical and pathological features of aortic thrombolism in 36 dogs. J. Vet. Emerg Crit Care 1993; 30: 13-20.

개에서 다중나선형 CT촬영에 의한 동맥혈전색전증의 평가

신승호 · 이기창[1]

전북대학교 수의과대학

요 약 : 호흡곤란과 후지마비 및 발등부위의 괴사를 나타낸 수컷 진돗개가 전북대학교 동물의료센터에 내원하였다. 초기 검사에서 심장 사상충 감염이 확인되었다. 흉부방사선 외측상에서 폐동맥의 확장과 후엽의 간질패턴, 그리고 복배상에서 주 폐동맥의 뚜렷한 확장등이 관찰되어 심장사상충증을 뒷받침하였고, 복부 외측상 및 복배상에서 복부세부음영 소실이 관찰되어 복수를 의심하였다. 초음파상에서 복수와 불규칙한 간변연 그리고 신장양극의 피질에서 쐐기모양의 국소적 고에코상을 관찰하였으며 복부대동맥에서 분지하여 주행하는 바깥장골동맥의 3상형 동맥파형이 분지부 근위에서 관찰되었으나 이 후 대퇴동맥의 파형은 확인되지 않았다. 혈액화학검사에서 백혈구증다증, 빈혈, 혈색소 뇨, 고빌리루빈혈증, 저 알부민혈증, 전해질불균형, 그리고 간장 및 신장효소치의 상승등이 관찰되어 광범위한 장기의 손상이 의심되었다. 특히 글루코스는 정상적인 전지와 마비를 보이는 후지에서 비교한 결과 후지의 글루코스 수치가 현저하게 낮았다. 전산화단층촬영술 후 3차원으로 재구성한 영상을 이용하여 후지 마비의 원인으로 여겨지는 후지 동맥의 혈전색전증과 폐동맥혈전색전증 및 신장경색 등을 확인하였다. 예후불량으로 판단되었으며 실험적 중재적 방사선술을 시도하였으나 마취에서 깨어나지 못했다. 3차원 재구성 CT 영상은 색전증의 빠르고 정확한 진단에 유용하며 효과적인 치료 계획을 수립하는데도 큰 도움이 된다고 판단된다.

주요어 : 3차원 재구성영상, 혈전색전증, 심장사상충, 개